Semiconductor Physics, Quantum Electronics & Optoelectronics. 2004. V. 7, N 2. P. 185-189.

PACS: 78.67.-n; 78.67.Bf; 78.40.-q; 78.40.Fy

Growth and linear optical properties of CuCl nanocrystals

S. Mahtout, M.A. Belkhir, M. Samah

Group of Solid State Physics, University of Bejaia, 06000 Bejaia, Algeria. E-mail: mahtout_sofiane@yahoo.fr

Abstract. Linear optical properties of CuCl nanocrystals in a NaCl matrix have been studied using optical absorption, cathodoluminescence and X-ray diffraction measurements. Our measurements showed that CuCl nanocrystals were really formed. Their average size was estimated to be 2.2 nm. Consistently with confinement effect resulting from the low size of the nanocrystals, a blue shift of excitonic levels is observed by comparison to the bulk crystal. Our analysis showed that the effect of thermal annealing depends on the temperature, the annealing time and the nature of cooling.

Keywords: nanocrystals, CuCl, exciton, confinement.

Paper received 13.02.04; accepted for publication 17.06.04.

1. Introduction

Many semiconducting materials that precipitate such as clusters on a nanometer scale in dielectric matrix, glass or polymers, have been recently studied [1–8]. This type of materials offers the possibility for optical investigation of new quantum confinement effect. A quantum confinement effect on the CuCl quantum dots (QD) is explained in terms of the excitons confinement regime [9,10], i.e. weak confinement. In our case, to fabricate these CuCl materials, we used a NaCl crystalline matrix which is transparent in the visible and near UV ranges. The CuCl nanocrystals were obtained by doping the matrix, during growth, with a fine powder of copper using the Czochralski method [11].

In order to characterize CuCl nanocrystals, the optical properties of CuCl nanocrystals were first examined using a linear absorption technique. The effect of thermal annealing for various temperatures, lower (300°C) and higher (500°C and 700°C) than the CuCl melting point (440°C), as that of the nature of cooling were also studied. Cathodoluminescence measurements at ambient temperature and X-ray diffraction (XRD) were then performed.

2. Experiment

As crystal growth method, we utilized the Czochralski technique. The grown samples (thicknesses ≈2 mm and surface ≈1 cm^2) were cleaved from NaCl single crystals doped during growth by a fine powder of copper. Doping of the melted NaCl was done at temperature averaging 900°C which is higher than the melting point of NaCl. Chosen pulling parameters were 1cm/h and 1tr/mn respectively for translation and rotation movements. Due to the rotation of the seed crystal the concentration gradient is not only longitudinal but also radial. Mixtures of NaC1 and CuC1 show a behaviour which is typical for a phase diagram with an eutectic temperature reported to be about 300°C [12].

3. Results and discussions

Optical absorption measurements were performed, on several samples, at ambient temperature in the range wavelengths going from 200 nm to 600 nm corresponding to the visible part of the NaCl matrix. The results are represented in Figure 1,*a*. Several peaks are observed in the transparent zone of the matrix. The absorption peak at about 254 nm has been assigned to the internal electronic transitions of Cu^+ [13,14]. The very fine peak which appears at 360 nm is due to the change of the lamp of the measuring equipment. The spectrum of Figure 1,*b* is the absorption spectrum of the CuCl nanocrystals formed in NaCl matrix. In this absorption spectrum, we can observe two peaks at about 368.5 nm (3.365 eV) and 372.5 nm (3.328 eV) which are assigned to $Z_{1,2}$ and Z_3 excitons of CuCl, respectively.

The excitons are formed by an electron in the lowest conduction band (symmetry Γ_6, notation by Koster et al.

[15]) and a hole either in the upper most twofold-degenerate Γ_7 valence band (Z_3 exciton) or in fourfold-degenerate Γ_8 valence band ($Z_{1,2}$ exciton) [16]. This proves the formation of CuCl nanocrystals in the NaCl matrix. Due to confinement effect, the energy positions of these excitons are blue-shifted compared to excitons in bulk crystal as reported by several authors [17–19].

As a consequence of quantum confinement effect, the energy of an exciton confined in a spherical QD is expressed as follows [20,21]:

$$E = E_g - E_{ex} + \frac{\hbar^2 \pi^2}{2Ma^2}, \quad (1)$$

where E is the Z_3 exciton energy, E_g = 3.4 eV the band gap energy of bulk CuCl crystal, $\hbar$ the Planck constant, M the translational mass of exciton, and a the average radius of nanocrystals. The binding energy of exciton is given by:

$$E_{ex} = \frac{\hbar^2}{2\mu a_B^2},$$

where μ is the reduced mass of the electron-hole system and a_B is the Bohr radius of exciton given in SI units by:

$$a_B = \frac{4\pi\varepsilon_0 \varepsilon \hbar^2}{\mu e^2},$$

where ε_0 is the permittivity of the vacuum, ε the dielectric constant of CuCl and e the absolute electronic charge. Here we took E_{ex} = 190 meV given in reference [22]. Using equation (1) the diameter ($2a$) of nanocrystals was estimated to be 2.25 nm taking account the Z_3 exciton position [23]. In the visible part of the spectrum of Figure 1,*a*, exhibits two peaks at 435 nm and 469 nm (Fig. 1,*c*). According to Dikjen et al. [24], these transitions are due to trap levels located in the gap of CuCl nanocrystals.

The study of annealing effect was performed on several samples at various temperatures (300°C, 500°C and 700°C). Figure 2,*a* shows, through curve 1 and 2, the evolution of the absorption spectrum as a function of the annealing time, at 300°C. Curve 1 corresponds to the rough sample, i.e. before annealing, and curve 2 is the spectrum after 24 hours of annealing. During the different stages, cooling is done in an abrupt manner at the ambient temperature. The evolution of spectrum shows a progressive diminution of the peak corresponding to copper and the appearance of another peak at 340 nm. The latter one is magnified in Figure 2,*b*. Table 1 illustrates this evolution for various stages of annealing. From this particular behaviour, we allot this peak to a compound based copper (*cbc*).

It is known that if the size of CuCl particles increases, the Z_3 exciton peak position moves toward the low energy side because of the quantum confinement effect [20,21, 25,26]. Thus, the shift of the Z_3 exciton peak toward the low energy side is attributed to the increase of the CuCl particles mean size with the annealing time. In our case, we observe a shift of the $Z_{1,2}$ peak from 368 nm to 369.5 nm and the shift of the Z_3 exciton peak from 372 nm to 375.5 nm. This is a consequence of an increase in the size of CuCl nanocrystals. Indeed, one finds, from equation (1), that the size passes from 2.2 to 2.6 nm.

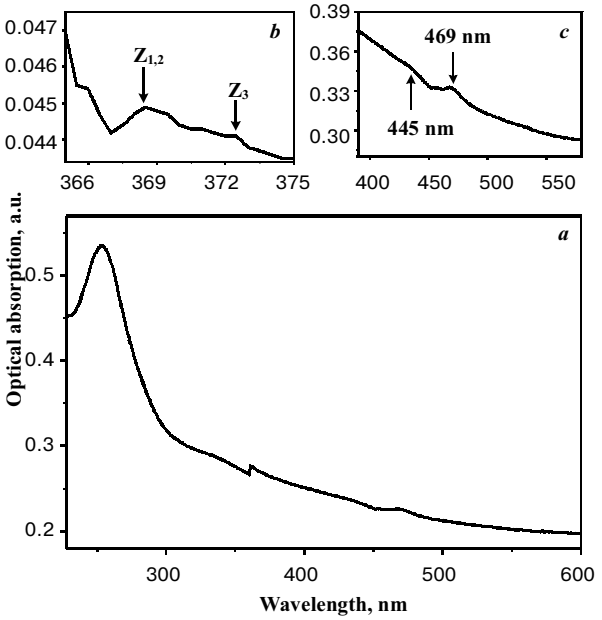

Fig. 1. *a* – optical absorption spectrum of NaCl doped by copper; *b* – optical absorption spectrum of CuCl nanocrystals; *c* – emission of trap levels in NaCl doped by copper.

Figure 3,*a* shows, through curve 1 and 2, the evolution of the optical absorption spectrum of another sample which has undergone a thermal annealing during sev-

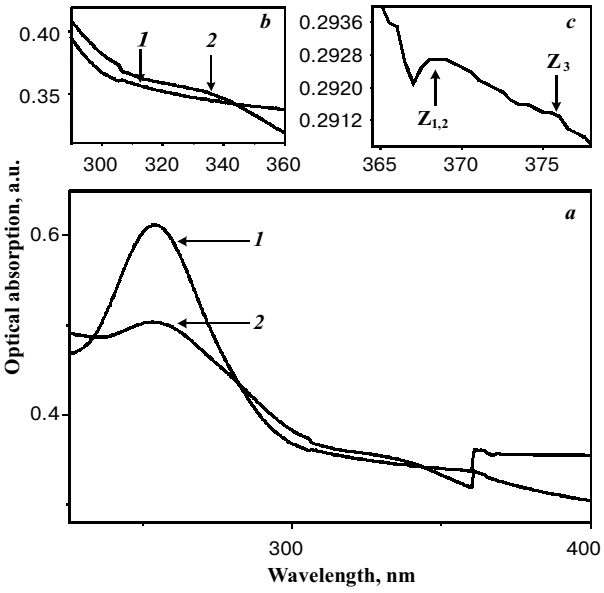

Fig. 2. *a* – evolution of the optical absorption spectrum according to the annealing time at 300°C: (1) rough sample; (2) after 24 hours of annealing. *b* – magnification of the zone around the peak at 340 nm. *c* – optical absorption spectrum of CuCl nanocrystals after 24 hours of annealing at 300°C.

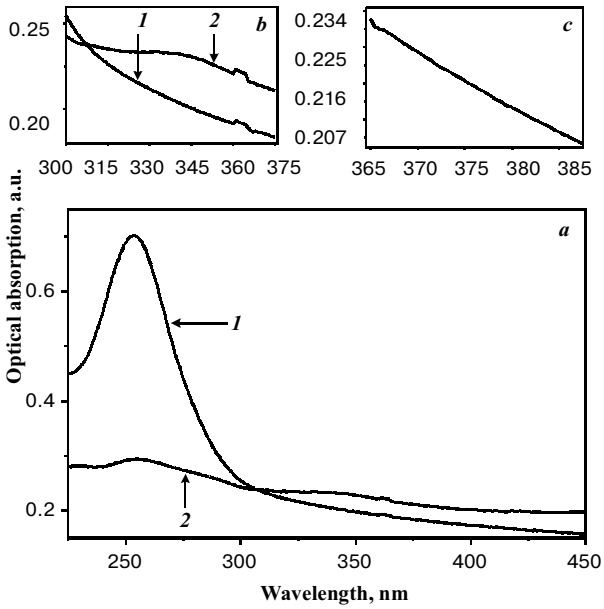

Fig. 3. *a* – evolution of the optical absorption spectrum according to the annealing time at 500 °C: (1) rough sample, (2) after 24 hours of annealing; *b* – magnification of the zone around the peak at 340 nm; *c* – optical absorption spectrum of CuCl nanocrystals after 24 hours of annealing at 500°C.

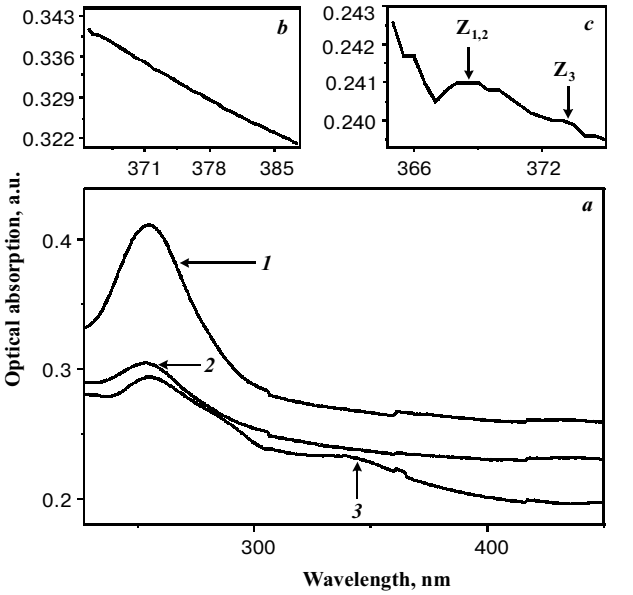

Fig. 4. *a* – Evolution of the optical absorption spectrum according to the annealing time at 700°C: (1) rough sample, (2) after 12 hours of annealing, (3) after 24 hours of annealing; *b* – optical absorption spectrum of CuCl nanocrystals after 12 hours of annealing at 700°C; *c* – optical absorption spectrum of CuCl nanocrystals after 24 hours of annealing at 700°C.

eral stages at 500°C. Curve 1 corresponds to the rough sample, i.e. before annealing, and curve 2 is the spectrum after 24 hours of annealing. Cooling is once again done in an abrupt manner at the ambient temperature. As can be seen from Figure 3,*b* and table 2, a similar behaviour as that at 300 °C, is observed. This is consistent with the fact that the compound contains copper. Figure 3,*c* shows the optical absorption spectrum of CuCl nanocrystals after 24 hours of annealing. We observe a disappearance of $Z_{1,2}$ and Z_3 peaks corresponding to CuCl excitons. This is due to the melting of CuCl nanocrystals because of their low melting temperature (440°C) compared to that of the furnace (500°C).

Another series of annealing was made on another sample at 700°C. This time, two types of cooling were adopted. For the first stage, cooling is abrupt at ambient temperature and for the other stage, cooling is 12 hours long. The evolution of the spectrum is represented in Figure 4,*a*. In the spectrum 2 (abrupt cooling), no peak appears in the spectrum except that corresponding to copper at 254 nm. Indeed, as shown in Figure 4,*b*, no peak appears in the excitonic resonance zone of CuCl after 12 hours of annealing. The explanation is as follows. Because of the high temperature of annealing (700°C), all the compounds in the sample are dissociated due to their low melting point (440 °C for CuCl) and then the abrupt cooling leaves the different constituents in their dissociated state. In the spectrum 3, cooling is very long, i.e., the temperature goes from 700°C to 500°C during the first two hours, then from 500°C to 300°C during the following 4 hours and finally from 300°C to ambient temperature during the remaining six hours. As can be seen in the spectra, several peaks appear, in particular the one at 340 nm and the $Z_{1,2}$ and Z_3 excitons peaks (Fig. 4,*c*)

Table 1. Evolution according to time of the cbc peak with respect to the Cu peak at 300°C.

Time, h	Peak Cu, a.u.	Peak cbc/Peak Cu
0	0.6124	0.5452
8	0.5884	0.5781
12	0.5724	0.6163
16	0.5469	0.6328
24	0.5039	0.6945

Table 2. Evolution according to time of the cbc peak with respect to the Cu peak at 500°C.

Time, h	Peak Cu, a.u.	Peak cbc/Peak Cu
0	0.7009	0.2939
8	0.4954	0.3982
12	0.4524	0.6096
16	0.4094	0.7774
24	0.2995	0.7923

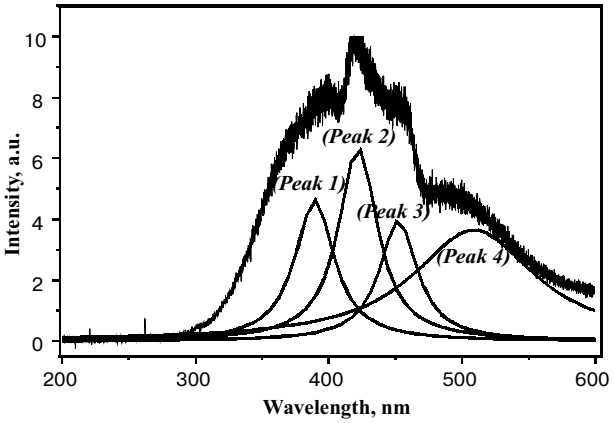

Fig. 5. Cathodoluminescence spectrum of NaCl doped with copper.

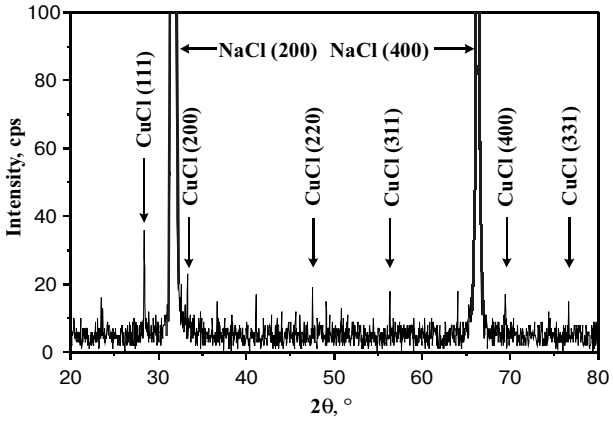

Fig. 6. XRD spectrum of NaCl doped with copper.

after 24 hours of annealing) of CuCl. These peaks are due to the long duration of cooling. In other words, when the temperature of the furnace passes under the melting point of the materials to be formed, the latter are formed by interaction of the various components of the samples. Using equation (1), the average diameter ($d = 2a$) of the formed CuCl nanocrystals was estimated to be 2.3 nm.

Cathodoluminescence is a method conventionally used to analyze the crystal structure of a specimen [27], including trace impurities, lattice defects and crystal distortion. In our case, measurements were made on a sample of NaCl doped with copper, at ambient temperature, with 5 eV electron beam energy. The obtained spectrum is represented in Figure 5. The deconvolution of the curve shows the existence of 4 peaks noted Peak1, Peak2, Peak3 and Peak4. The first one is at 389 nm. To explain the origin of this peak, we compared it to that of the emission spectrum, at liquid nitrogen temperature (77°C), of NaCl doped by copper [7]. This spectrum showed a CuCl nanocrystals emission peak which is practically at the same position than Peak1. Correspondingly, this peak is attributed to the emission of CuCl nanocrystals. Peak2 is located at 423 nm. According to Patil *et al.* [28] and Kurobori et al. [29], this one is attributed to the emission of the impurity atoms in the NaCl matrix as copper complexed with OH- (Cu+-OH-). Indeed, these authors observed a band at 420 nm in the luminescence spectrum of NaCl doped by copper. By analogy with the results of optical absorption, Peak3 and Peak4, located at 451 nm and 509 nm, are probably due to trap levels emission caused by defects formed in the CuCl nanocrystals.

XRD measurements were taken on several samples and the obtained spectra are all identical. Let us note that, by using a monochromator, only the line K_α of copper was selected from the source of X-rays. The spectrum of Figure 6 presents an example of these results. It consists of two principal lines on positions $2\theta = 31.68°$ and $2\theta = = 66.24°$. The first corresponds to the diffraction plane family (200) of NaCl and the second to its harmonic (400). The appearance of these two harmonics confirms the good monocrystallinity of the fabricated matrix. The lower intense lines, appear at $2\theta = 28.39°$, $2\theta = = 33.32°$, $2\theta = 47.52°$, $2\theta = 56.32°$, $2\theta = 69.44°$ and $2\theta = = 76.68°$, corresponding to the plane families diffraction (111), (200), (220), (311), (400) and (331) respectively of a CuCl crystal structured zincblende. This result confirms the presence of CuCl nanocrystals in the matrix.

In summary, Czochralski technique was employed to fabricate CuCl nanocrystals in NaCl matrix. Our measurements confirm that CuCl nanocrystals were really formed. The average diameter of nanocrystals was estimated to be 22 Å. As a consequence of confinement effect, it was observed a blue-shift of exciton positions. It is shown that the thermal annealing effect led to an increase in the nanocrystals mean size, when the annealing temperature is lower than the melting point of CuCl. On the other hand, for temperature higher than the melting point of CuCl, the effect of thermal annealing depends on the nature of cooling. That is, when cooling is abrupt there is disappearance of CuCl and when it is long it leads to the appearance of CuCl nanocrystals.

References

1. E. Rabani, B. Hetenyi, B.J. Berne and L.E. Brus // *J. of Chemical Physics*, **110**, No. 11, pp. 5355-5369 (1999).
2. J. Zhao, M. Ikezawa, A.V. Fedorov and Y. Masumoto // *J. of Luminescence*, **87-89** (2000), 525-527.
3. H.A. Ali, A.A. Iliadis, R.F. Mulligan, A.V.W. Cresce, P. Kofinas and U. Lee // *Solid-State Electronics*, **46** pp. 1639-1642 (2002).
4. H. Yang, X. Wang, H. Shi, F. Wang, X. Gu and X. Yao // *J. of Crystal Growth*, **236**, 371-375 (2002).
5. A.A. Lipovskii, E.V. Kolobkova and V.D. Petrikov // *J. of Crystal Growth*, **184/185**, pp. 365-369 (1998).
6. N. Thantu, R.S. Schley and B.L. Justus // *Optics Communications*, **220**, pp. 203-210 (2003).
7. T. Kawazoe and Y. Masumoto // *Phys. Rev. Lett.*, **77**, pp. 4942-4945 (1996).
8. M. Haselhoff and H.-J. Weber // *Phys. Rev. B*, **58**, pp. 5052-5061 (1998).
9. T. Itoh, Y. Iwabuchi and M. Kataoka // *Phys. Stat. Sol. (b)*, **145**, P. 567 (1988).
10. Y. Kayanuma // *Phys. Rev. B*, **38**, 9797 (1988).

11. J. Czochralski, Ein neues Verfahren zur Messung der Kristallisationsgeschwindigheit der Metalle // *Z. phys. Chemie*, **92**, pp. 219-221 (1918).
12. M. Haselhoff and H.-J. Weber // *Material Research Bulletin*, **30**, No.5, pp. 607-612 (1995).
13. S. Nagasaka, M. Ikezawa and M.Veta // *J. Phys. Soc. Japan*, **20**, pp. 1450 (1995).
14. H. Kishishita // *Phys. Stat. Sol. (b)*, **55**, pp. 399 (1973).
15. G.F. Koster, J.O. Dimmoch, R.G. Wheeler and H. Statz, *Properties of the thirty-two point groups* // MIT Press, Cambridge, MA (1963).
16. V. Albe, *These de Doctorat de l'Universite de Montpellier II*, France (1997).
17. S. Park, I. Kim, K. Jang, S. Kim, C. D. Kim, Y. Yee and G. Jeen // *J. Phys. Soc. Jpn.*, **70**, No. 12, pp. 3723-3727 (2001).
18. M. Cordona // *Phys. Rev.*, **129**, pp. 69 (1963).
19. H. Ohmura and A. Nakamura // *J. of Luminescence*, **76&77** pp. 125-129 (1998).
20. A.I. Ekimov, Al.L. Efros and A.A. Onushchenko // *Solid State Commun*, **56**, pp. 921 (1985) .
21. A.I. Ekimov, A.A. Onushchenko, A.G. Plyukhin and Al.L. Efros // *Sov. Phys.-JETP*, **61**, pp. 991 (1985).
22. Landoft-Bornstein, *Zahlenwerte and Funktionen aus Naturwissenschaft and Technik*, Neue Seie, Springer, Berlin (1987), Band III/22a.
23. M. Haselhoff, K. Reimann and H.-J. Weber // *J. Of Crystal Growth*, **196**, pp. 135-140 (1999) .
24. A. Van Dijken, E.A. Meulenkamp, D. Vanmaekelbergh and A. Meijerink // *J. Of Luminescence*, **90**, pp. 123-128 (2000).
25. T. Itoh, Y. Iwabuchi and T. Kirihara // *Phys. Status Solidi B*, **146**, pp. 531 (1988) .
26. A.I. Ekimov and A.A. Onushchenko // *JETP Lett.*, 34 pp. 347 (1981).
27. B.G. Yacobi and D.B. Holt // *J. Appl. Phys.*, **59**(4), pp. R1-R24 (1986).
28. R.R. Patil and S.V. Moharil // *J. of Luminescence*, **63**, pp. 339-344 (1995).
29. T. Kurobori, S. Taniguchi and N. Takeuchi // *J. of Luminescence*, **55**, pp. 183-186 (1993).